An offshore wind energy conversion system based on a Permanent Magnet Synchronous Generator connected to Grid -Modeling and Control Strategies

Morlaye Sekou Camara; Mamadou Baïlo Camara, *Member IEEE;* Brayima Dakyo, *Member IEEE*
Laboratoire GREAH - Université Le Havre
25 Rue Philippe Lebon, 76058 Le Havre, FRANCE
Email: camarasekou2012@gmail.com, camaram@univ-lehavre.fr, brayima.dakyo@univ-lehavre.fr

Hamid Gualous, *Member IEEE*
Laboratoire LUSAC – Université de Caen
Rue Louis Aragon, 50100 Cherbourg - Octeville, FRANCE
Email: hamid.gualous@unicaen.fr

***Abstract*— This paper presents modeling and control strategies of 5MW Permanent Magnet Synchronous Generator (PMSG) for offshore wind energy conversion application. The PMSG is connected to electrical grid of 20kV phase to phase *RMS* voltage using a back-to-back converter.**

The contribution of this paper is focused on energy management strategies using "grid code", where the required power profile is fixed by electrical grid manager without any consideration for wind speed variations. For this study, it is assumed that the available power is higher than required power for electrical grid. The proposed control strategies include a Maximum Power Tracking (MPPT) for PMSG speed control, active/reactive power control, and DC-bus voltage management. To show the performances of the control, some simulation results are presented and analyzed using Matlab/Simulink software.

Keywords*— Active and reactive power control; AC/DC converter; DC/AC converter; DC-bus voltage control; Permanent Magnet Synchronous Generator (PMSG); Offshore wind energy management; Speed control; Maximum Power Point Tracking (MPPT); Wind energy conversion.

I. INTRODUCTION

The industry of wind generators knew has spectacular growth during these last years. Before, the wind generators power does not reach in order of megawatts. For this reason, the major part of first models is based on Permanent Magnet Synchronous Generators (PMSG) or conventional asynchronous generator. The conventional asynchronous generators are generally connected to turbine through a gear box. PMSG can be coupled to turbine via a gear box or directly without a gear box if the generator has a high number of poles [1], [2]. Due to power increase until to megawatts (10 MW today), the PMSG configuration necessitates an increasing of size and weight of converters.

Permanent magnet synchronous generators compared to conventional generators have the advantages of being robust in construction, very compact in size, not requiring an additional power supply for magnetic field excitation, and requiring less maintenance. A variable speed wind energy conversion system including a PMSG offers advantages over the constant speed approach, such as maximum power point tracking capability and reduced acoustic noise at lower wind speeds [3-4].

The contribution of this paper is focused on energy management strategies using "grid code", where the required power profile is fixed by electrical grid manager without any consideration for wind speed variations. The PMSG is linked to electrical grid using a back-to-back converter as illustrated in Fig.1, where electrical grid presents phase to phase *RMS* voltage of 20kV. Proposed control strategies include a Maximum Power Point Tracking (MPPT) for PMSG speed control, the active/reactive power control, and DC-bus voltage control management. To show the performances of control strategies, some simulation results are presented and analyzed using Matlab/Simulink software.

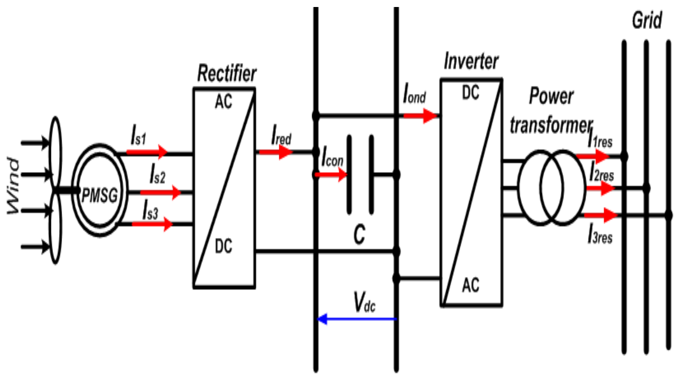

Fig.1: Wind energy conversion system using Permanent Magnet Synchronous Generator.

II. Wind Energy Convers System Modelig

A. *Wind turbine modeling*

Theoretical power due to wind turbine is given in (1), where ρ presents air density; S is the circular area swept by turbine; β is blades pitch angle, v presents wind speed in [m/s], [5].

$$P_t = \frac{1}{2} \cdot C_p(\lambda, \beta) \cdot \rho \cdot S \cdot v^3 \qquad (1)$$

The ratio between tip speed of the turbine and wind speed is expressed in (2), where Ωm is the speed of turbine; Rt is the radius of the wind turbine.

$$\lambda = \frac{\Omega_m \cdot R_t}{v} \qquad (2)$$

The power coefficient C_p can be estimated using (3), [6].

$$\begin{cases} C_p(\lambda, \beta) = (0.35 - 0.00167 \quad) \cdot (\beta - 2) \cdot \sin(A) \\ - 0.00184 \quad \cdot (\lambda - 3) \cdot (\beta - 2) \\ A = \dfrac{\pi \cdot (\lambda + 0.1)}{14.34 - 0.3(\beta - 2)} \end{cases} \qquad (3)$$

The mechanical torque C_m of wind turbine obtained from (1) is expressed in (4).

$$C_m = \frac{P_t}{\Omega_m} \qquad (4)$$

The mechanical equation can be expressed as presented in (5), where J_t and J_m present respectively the inertia moments of the turbine and the generator; fv is the coefficient due to viscous rubbings of generator; Ω_m is the generator speed.

$$(J_t + J_m) \cdot \frac{d\Omega_m}{dt} + f_v \cdot \Omega_m = C_m - C_{em} \qquad (5)$$

B. *PMSG modeling*

The PMSG dynamic model in *dq* axis can be writing as presented in (6); where R_s is the resistance in stator; and L_d and L_q are the stator inductances in *dq* axis ; I_{sd} and I_{sq} present the currents in stator; φ is the permanent magnet flux, p is the pair poles, [7].

$$\frac{d}{dt}\begin{bmatrix} I_{sd} \\ I_{sq} \end{bmatrix} = \begin{bmatrix} -\dfrac{R_s}{L_d} & \dfrac{p \cdot \Omega_m \cdot L_q}{L_d} \\ -\dfrac{p \cdot \Omega_m \cdot L_d}{L_q} & -\dfrac{R_s}{L_q} \end{bmatrix} \cdot \begin{bmatrix} I_{sd} \\ I_{sq} \end{bmatrix} + \begin{bmatrix} \dfrac{V_{sd}}{L_d} \\ \dfrac{V_{sq} - p \cdot \Omega_m \cdot \varphi}{L_q} \end{bmatrix} \qquad (6)$$

In this paper, smoothed poles PMSG is considered for system simulations which enables to write $L_d = L_q = L_s$.

C. *Back-to-back converter modeling*

This section presents the three phase back-to-back converter (rectifier and inverter) analytical model. Based on Fig.1, the measured currents in DC-bus can be expressed as presented in (7), where C is the DC-bus capacitor; I_{ond} is the inverter input current; I_{s1}, I_{s2} and I_{s3} present the rectifier input currents.

$$\begin{cases} I_{red} = S_a \cdot I_{s1} + S_b \cdot I_{s2} + S_c \cdot I_{s3} \\ C \cdot \dfrac{dV_{dc}}{dt} = I_{red} - I_{ond} \end{cases} \qquad (7)$$

Analytical model of inverter is given in (8), where, V_{dc} is the DC-bus voltage, w_1, w_2 and w_3 present the three phase PWM (pulse with modulation) signals applied to inverter.

$$\begin{cases} V_{Sa} = \dfrac{2 \cdot w_1 - w_2 - w_3}{3} \cdot V_{dc} \\ V_{Sb} = \dfrac{2 \cdot w_2 - w_1 - w_3}{3} \cdot V_{dc} \\ V_{Sc} = \dfrac{2 \cdot w_3 - w_1 - w_2}{3} \cdot V_{dc} \end{cases} \qquad (8)$$

D. *Electrical grid model*

The goal of this section consists to establish an ideal model of electrical grid. To establish this model, the balanced three phase system is considered, where V_{1res}, V_{2res} and V_{3res} are connected to inverter through a transformer with ratio of m. Based on Fig.2, the analytical model of electrical grid is presented in (9), where e_1, e_2 and e_3 present the conventional three phase *emf* with phase to phase *RMS* voltage of 20kV.

$$\begin{cases} V_{1res} - e_1 = R_{res} \cdot I_{1res} + L_{res} \cdot \dfrac{d}{dt}(I_{1res}) \\ V_{2res} - e_2 = R_{res} \cdot I_{2res} + L_{res} \cdot \dfrac{d}{dt}(I_{2res}) \\ V_{3res} - e_3 = R_{res} \cdot I_{3res} + L_{res} \cdot \dfrac{d}{dt}(I_{3res}) \end{cases} \qquad (9)$$

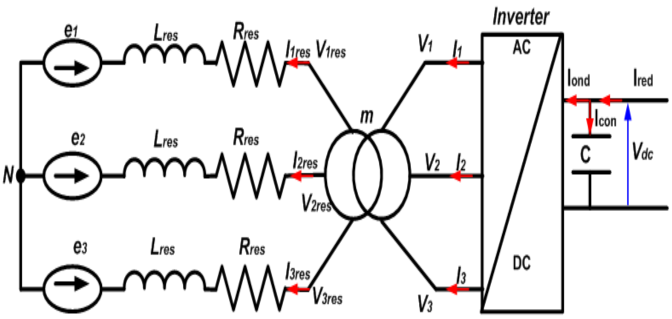

Fig2: Ideal model of electrical grid.

III. OFFSHORE WIND ENERGY SYSTEM CONTROL STRATEGIES

Adopted control strategies are focused on: - PMSG speed control based on the Maximum Power Point Tracking (MPPT) technique; - active and reactive power control using inverter; - DC-bus voltage control through rectifier connected to stator. Similar methods are described in [8], [9], [10], [11], [12] and [13].

A. *PMSG Speed control strategy*

To control PMSG speed, the wind turbine speed reference is expressed in (10), where *v* presents the wind speed. This reference is obtained from MPPT technique.

$$\Omega_{refw} = \frac{\lambda_{opt} \cdot v}{R_t} \tag{10}$$

The PMSG speed control strategy is illustrated in Fig.3. PI controller coefficients obtained from closed loop analysis are expressed in (11), where ω_{nd} and t_{sd} are respectively the dynamics of the system and the system time constant, [14].

$$\begin{cases} K_p = \sqrt{2} \cdot \omega_{nd} \cdot J \\ K_i = \omega_{nd}^2 \cdot J \end{cases}, \omega_{nd} = \frac{5.8}{t_{sd}}, \ J = J_t + J_m \tag{11}$$

Active and reactive power control strategy

The active and reactive power injected in electrical grid is expressed in (12), where (V_{dres},V_{qres}) and (I_{dres},I_{qres}) are respectively the grid voltage and current in *dq* axis.

$$\begin{cases} P = V_{dres} \cdot I_{dres} + V_{qres} \cdot I_{qres} \\ Q = V_{qres} \cdot I_{dres} - V_{dres} \cdot I_{qres} \end{cases} \tag{12}$$

The reactive and active power control strategies are presented in Fig.4. Used parameters in PI controllers for inner and outer loops are respectively presented in (13), where t_{ir} and t_p are respectively the inner and outer loops time constants.

$$\begin{cases} K_{pir} = \frac{2.197 \cdot L_{res}}{t_{ir}} \\ K_{iir} = \frac{2.197 \cdot R_{res}}{t_{ir}} \end{cases} \qquad \begin{cases} K_{pp} = \frac{t_{ir}}{t_p} \\ K_{ip} = 2.197 \cdot t_p \end{cases} \tag{13}$$

C- *DC-bus voltage control strategy*

DC-bus voltage control strategy is illustrated in Fig.5, where the reference's current I_{qref} is obtained from DC-bus voltage control loop. I_{dref} is fixed to zero to obtain a power factor of 1. Like to PMSG speed control, PI controller is used for DC-bus voltage management. The parameters of this controller can be estimated using (14), where ω_n and t_{sdc} are respectively the dynamics of the system, and system time constant.

$$\begin{cases} K_{pdc} = \sqrt{2} \cdot \omega_n \cdot C \\ K_{idc} = \omega_n^2 \cdot C \end{cases}, \qquad \omega_n = \frac{5.8}{t_{sdc}} \tag{14}$$

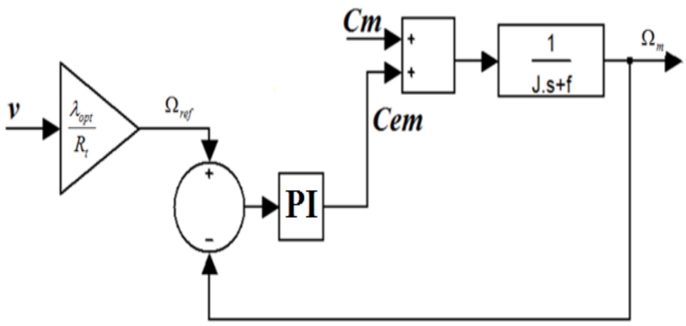

Fig.3: PMSG Speed control loop for wind turbine.

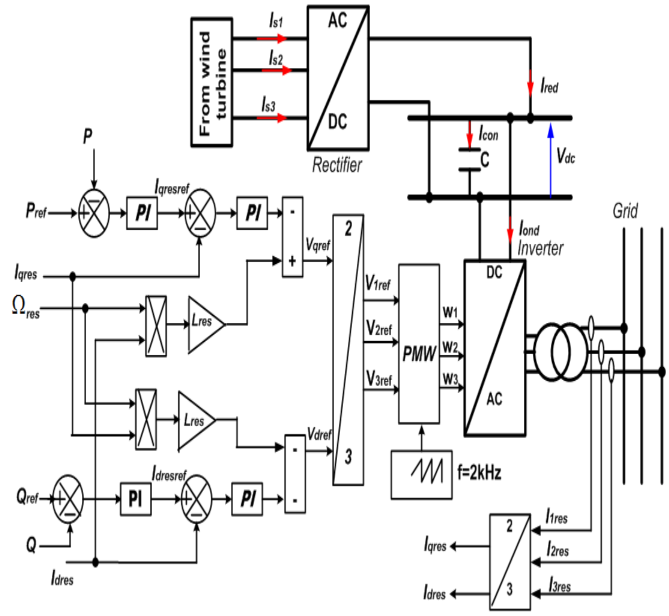

Fig4: Active and reactive power control strategies.

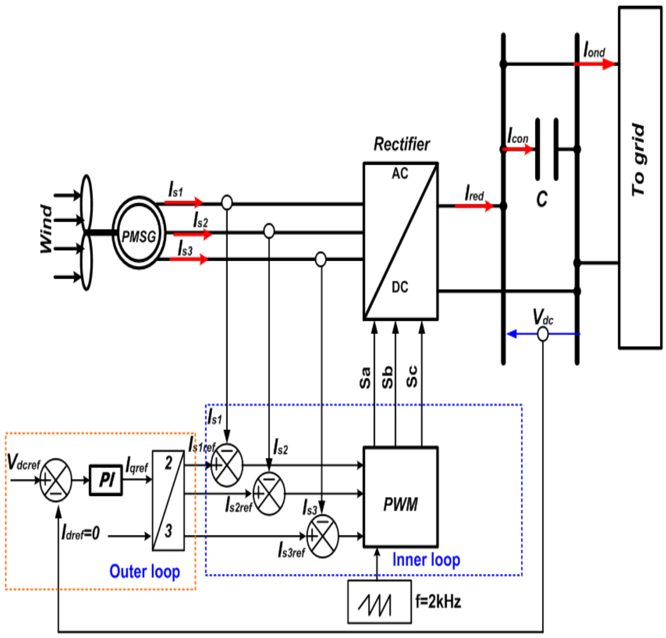

Fig.5: DC-bus voltage control strategy.

IV- SIMULATION RESULTS

Used parameters for system simulations are presented in Appendix section. The wind speed average value is fixed to 12m/s. The reference speed of wind turbine is estimated using (10). Based on “grid code”, the required power for electrical grid is illustrated in Fig.6. This profile is used as a reference for active power control. The reactive power reference Q_{ref} is estimated according to active power ones as expressed in (15), where $tg(\varphi)$ is respectively fixed to 0.327; 0 and -0.327. These conditions are fixed from electrical “grid code” described in [15], [16].

$$Q_{ref} = P_{ref} \cdot tg(\varphi), \begin{cases} tg(\varphi) = 0.327 \rightarrow Q_{ref} > 0 \\ tg(\varphi) = 0 \rightarrow Q_{ref} = 0 \\ tg(\varphi) = -0.327 \rightarrow Q_{ref} < 0 \end{cases} \quad (15)$$

To show the performances of control, DC-bus voltage reference is respectively fixed to 5kV and 6kV. By convention, the sign of reactive power is assumed positive for injected power, and negative for absorbed power.

Fig.7 shows the wind speed profile, where minimum and maximum values are respectively 8.9m/s and 15m/s. Wind turbine speed control result is presented in Fig.8. This curve shows that, the proposed control strategy is satisfactory, i.e. controlled speed is close to reference ones. The active and reactive powers control results are respectively presented in Fig.9 and Fig.10.These results allow to concluding the proposed control strategies are satisfactory. The controlled powers compared to references ones show that, the control strategies take into account the wind speeds variations. Fig.11 presents DC-bus voltage control result. This curve shows that, DC-bus voltage follows the fixed references (5kV and 6kV), which enables to conclude that, proposed control is performing except during initial conditions, where DC-bus voltage control loop has not enough time to react.

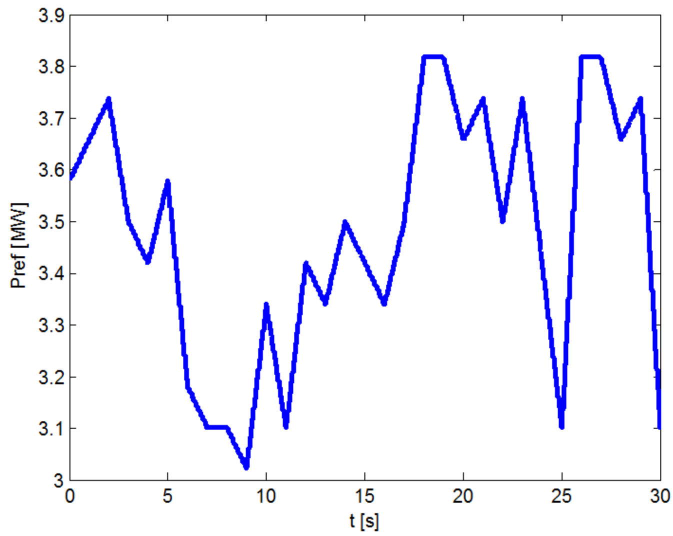

Fig.6: Required power for electrical grid based on “grid code”.

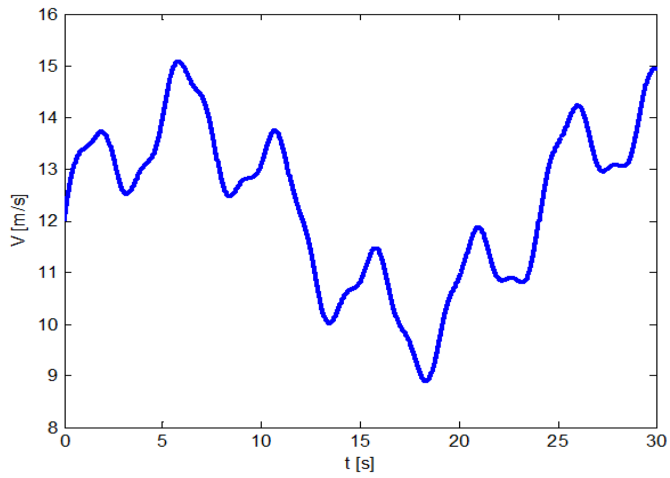

Fig.7: Used profile for wind speed.

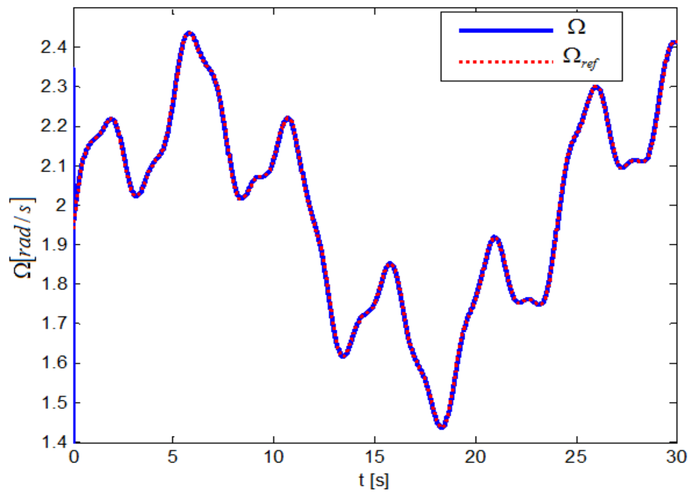

Fig.8: PMSG Speed control result.

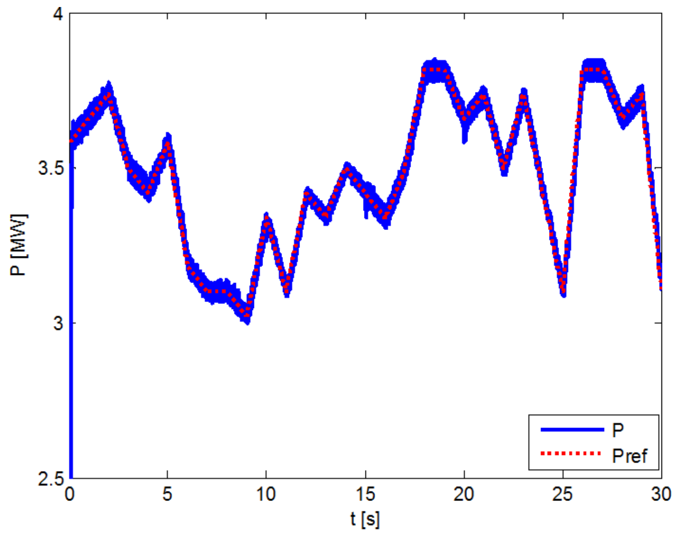

Fig.9: Active power control result.

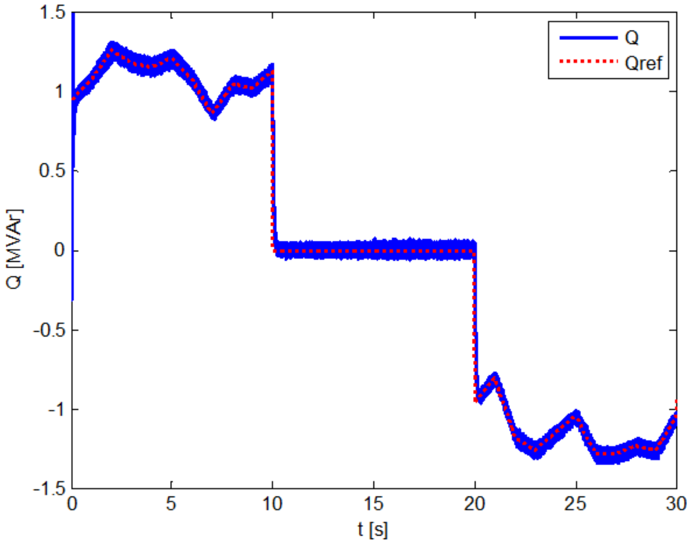

Fig.10: Reactive power control result.

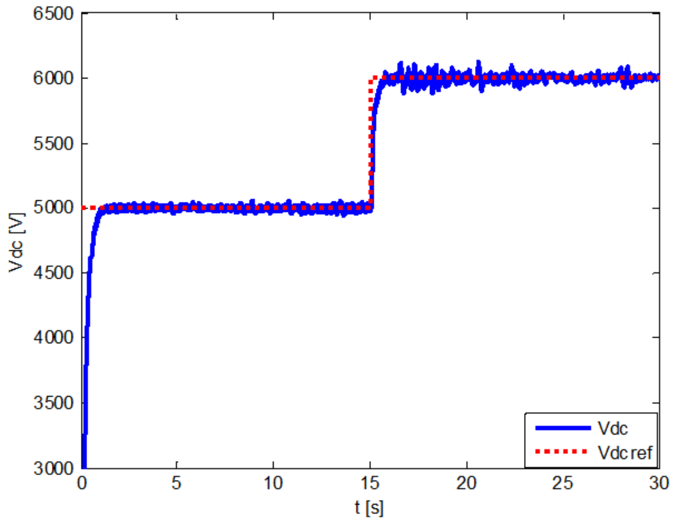

Fig.11: DC-bus voltage control result.

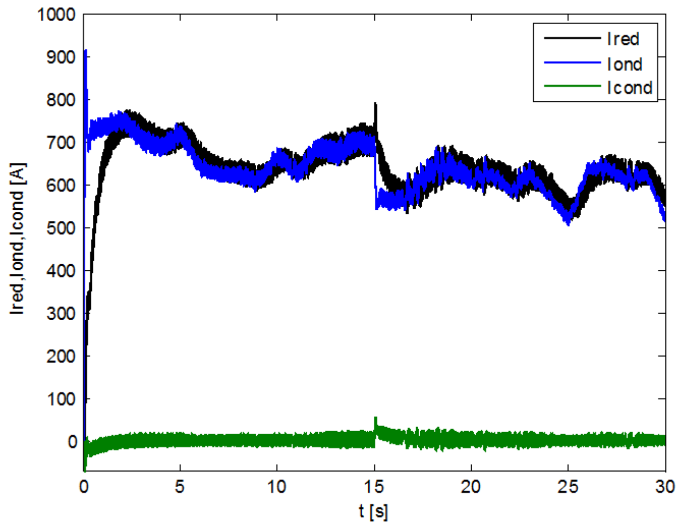

Fig.12: Measured currents in DC-bus.

The currents in DC-bus are presented in Fig.12. These curves show that, the contribution of wind turbine I_{red} is close to injected current in inverter I_{ond}, because DC-bus capacitor is charged during first operation.

V- CONCLUSION

In this paper, the authors present modeling and control strategies for offshore wind energy conversion system based on Permanent Magnet Synchronous Generators connected to electrical grid. Proposed control strategies are focused on PMSG speed control, DC-bus voltage management, and active/reactive power control. Simulation results show that, the proposed control strategies are satisfactory and controlled variables are very close to references ones. Based on this study, the PMSG seems to be interesting for offshore wind energy applications.

APPENDIX

TABLE I: PMSG Parameters

Parameters	Symbols	Values
Rated power	P_n	5 MW
RMS voltage in the stator	U_{sef}	3.3 kV
Resistance in stator	R_s	50 mΩ
Stator inductance	L_s	7.5 mH
Number of poles pair	p	60
PMSG inertia moment	J_m	$2x10^5$ kg.m^2
Magnetic induced flux	φ	28.6 Wb

TABLE II: Parameters of wind turbine

Parameters	Symbols	Values
Radius of wind turbine	R	60 m
Air density	ρ	*1.225 kg/m^3*
Optimal tip-speed ratio	λ_{opt}	9.7
Wind turbine inertia moment	J_t	$30*10^6$ kg.m^2
Maximum power coefficient	$C_p(\lambda_{opt})$	0.53

TABLE III: Parameters of DC-bus and Electrical grid

Parameters	Symbols	Values
DC-bus voltage reference	V_{dcref}	5 kV to 6 kV
DC-bus capacitor	C	25 *mF*
Grid resistance	R_{res}	60 Ω
Grid inductance	L_{res}	0.2 H
Phase to phase *RMS* voltage of electrical grid	*emf*	20 kV

REFERENCES

[1] M. Liserre and M. Molinas, "Overview of Multi-MW Wind Turbines and Wind Parks," IEEE Trans. Ind. Electron., vol. 58, no. 4, pp. 1081–1095, 2011.

[2] M.S. Camara, M.B. Camara, B. Dakyo, H. Gualous, "Permanent Magnet Synchronous Generators For Offshore Wind Energy System Linked To Grid -Modeling And Control Strategies", IEEE, 16th International Power Electronics and Motion Control Conference, PEMC2014, Antalya/Turkey, pp. 165-169. 21-24 September, 2014.

[3] C.E.A. Silva, D. S. Oliveira Jr., L.H.S.C. Barreto, R.P.T. Bascopé, "A Novel Three-phase Rectifier with High Power Factor for Wind Energy

Conversion Systems", Power Electronics Conf., 2009, COBEP '09, pp. 985-992.

[4] Sasi.c and G.Mohan, "Performance Analysis of Grid Connected Wind Energy Conversion System with a PMSG during Fault Conditions"International Journal of Engineering and Advanced Technology (IJEAT) ISSN: 2249 – 8958, Vol.2, no.4, April 2013.

[5] F. D. Bianchi, H. D. Battista, and R. J. Mantz, "Wind Turbine Control Systems: Principles, Modelling and Gain Scheduling Design", London Springer, 2007.

[6] B. Singh and S. Sharmay, "Stand-alone wind energy conversion system with an asynchronous generator," Journal of Power Electronics, vol. 10, no. 5, pp. 538-547. Sept. 2010.

[7] M.S. Camara, M.B.Camara, B. Dakyo, H. Gualous, "Modélisation et commande d'une génératrice synchrone à aimant permanent pour la production et l'injection des énergies offshore dans un réseau", SGE2014, ENS Cachan, 8 - 10 juillet 2014.

[8] Jordi Zaragoza, Joseph Pou, Antoni Arias, Cyril Spiteri, Eider Robles, Salvador Ceballos, "Study and experimental verifycation of control tuning strategies in a variable speed wind energy conversion system', Journal of Renewable Energy, vol.36, Issue 5, pp:1421–1430, May2011.

[9] D.Ikni, M.S. Camara, M.B.Camara, B. Dakyo, H. Gualous, "Permanent Magnet Synchronous Generators for Large Offshore Wind Farm Connected to Grid - Comparative Study between DC and AC Configurations", International Journal of Renewable Energy Research, Vol.4, No.2, 2014.

[10] M.S.Camara; M.B. Camara; B. Dakyo; H.Gualous," Modeling and Control of the Offshore wind energy system based on 5MW DFIG connected to grid", IEEE-AFRICON, pp.991-995; 2013.

[11] A.G. Sanchez, M.G. Molina, A.M. Rizzato Lede, "Dynamic Model of wind energy conversion system system with PMSG-based variable-speed wind turbines for power system studies", International Journal of Hydrogen Energy, vol.37, Issue 13, July 2012, pp: 10064–10069.

[12] M.O.F.Diallo, M.B. Camara , S. Youssef, H.Gualous, B. Dakyo, "Energetic capability Characterization of the Raz Blanchard area for the tidal turbine farm implementation", IEEE Inter. Conf., AFRICON, 9- 12 Sept.2013, Mauritius.

[13] M. A. Tankari, M.B.Camara, B. Dakyo, G. Lefebvre "Use of Ultracapacitors and Batteries for Efficient Energy Management in Wind-Diesel Hybrid System", IEEE Transaction on Sustainable Energy, ISSN:1949-3029, Vol. 4, No.2, pp.414-424, April. 2013.

[14] A. Tapia, G. Tapia, and J. Ostolaza, "Modeling and control of a wind turbine driven doubly fed induction generator," IEEE Trans. Energy Conversion, vol. 18, no. 2, pp. 194–204, 2003.

[15] J. Aho, R. Jessler, A. Syomushkin, E. Catz" Grid Code Compliance Support for Connecting Renewable Energy into Transmission Line using D-STATCOM System", CIGRE 2012.

[16] Cosmin E. Bănceanu, Iulian V, " Coordinated control of wind turbine" , Master Thesis, Dept. Energy Technology - Pontoppidanstræde 101 Aalborg , Univ. Aalborg , Denmark, 2011.